Supplemental Document

Optics Letters

Hybrid modes in a single thermally excited asymmetric dimer antenna: supplement

LOUBNAN ABOU-HAMDAN,[1,2] CLAIRE LI,[1,2] RIAD HAIDAR,[2] VALENTINA KRACHMALNICOFF,[1] PATRICK BOUCHON,[2,3] AND YANNICK DE WILDE[1,4]

[1] *Institut Langevin, ESPCI Paris, PSL University, CNRS, 1 rue Jussieu, F-75005 Paris, France*
[2] *DOTA, ONERA, Université Paris-Saclay, F-91123 Palaiseau, France*
[3] *e-mail: patrick.bouchon@onera.fr*
[4] *e-mail: yannick.dewilde@espci.fr*

Supplement DOI: https://doi.org/10.6084/m9.figshare.13643345

Parent Article DOI: https://doi.org/10.1364/OL.413382

Hybrid modes in a single thermally excited asymmetric dimer antenna: supplemental document

1. EXPERIMENTAL DETAILS

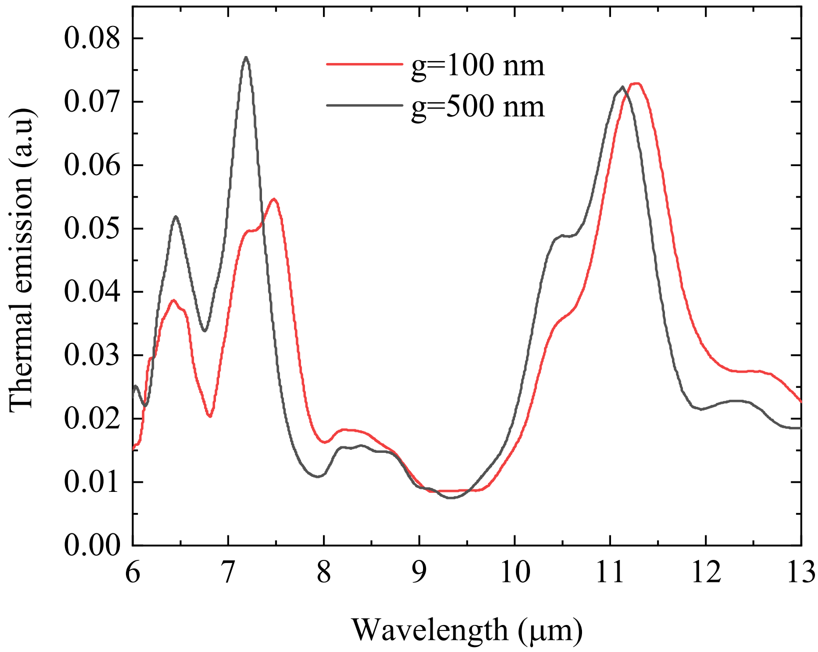

Fig. S1. Measured thermal emission spectra of the BiMIM structure for different gap sizes g (presented in Fig. 2 (a) of the main text), over the spectral range between 6–13 μm.

The infrared spatial modulation spectroscopy technique (IR-SMS) used to obtain the thermal emission of the isolated BiMIM structure is based on lateral modulation of the sample along with lock-in detection. The full details of the experimental technique have already been outlined elsewhere in Ref. [1]. The experimental setup is coupled to an FTIR which allows us to obtain the thermal emission spectra shown in Fig. 2(a) of the main text. For completeness, these spectra are again plotted here over the full spectral range of measurement between 6–13 μm in Fig S2.

During the measurements, the sample itself is the source of the thermal emission, which is brought upon by heating it to a uniform temperature. The presented measurements were performed at $T_{sample} = 438$ K. The instrumental response of the FTIR was calibrated with blackbody samples at different temperatures using the method outlined in Ref. [2]. The measured thermal emission spectra, presented in the main text, were normalized to the response of a blackbody at the same temperature to correct for instrumental response. As such, the normalized spectra are directly comparable to the emission cross-section of the BiMIM structure (see ref. [3] for more details).
To illustrate the fact that the IR-SMS technique allows one to obtain a better signal-to-noise ratio and can directly extract the thermal emission of the single BiMIM structure from the huge extended background radiation, we show in Fig. S2 raw (un-normalized) spectra of the BiMIM structure measured both using the IR-SMS technique and with a mechanical chopper. The two spectra are scaled according to the sensitivity used during the lock-in detection. As clearly indicated in Fig. S2 the signal coming from the sole BiMIM antenna, which is directly measured

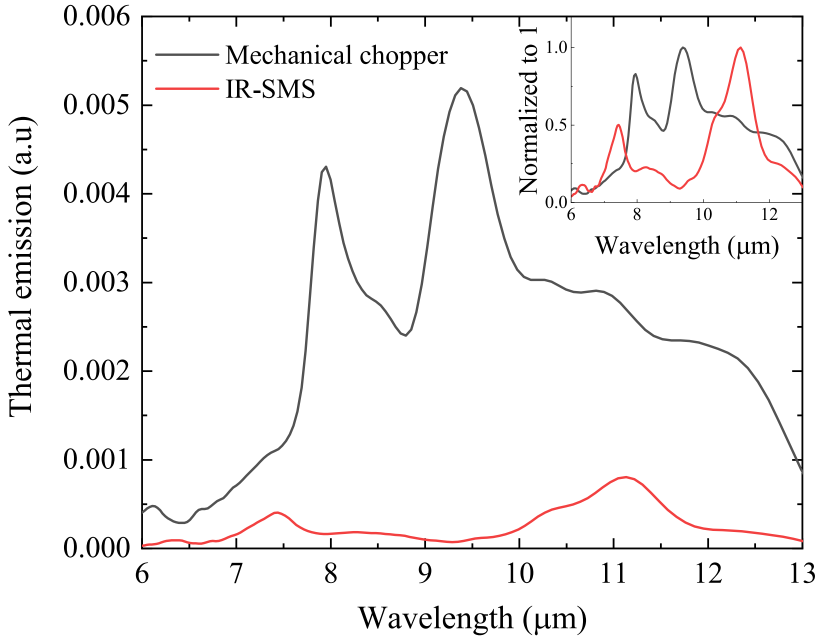

Fig. S2. Raw thermal emission spectra of the BiMIM structure measured using the IR-SMS technique and a mechanical chopper. The two spectra are scaled according to the sensitivity used in the lock-in detection. The inset shows a comparison of the two when normalized to 1.

by the IR-SMS technique, is much smaller than that of the background emission. On the other hand, the BiMIM emission is completely lost in the overwhelming signal coming from the substrate emission and background thermal radiation when the measurement is performed with a mechanical chopper. The peak near 9.5 μm in Fig. S2 (black curve) for instance, is an absorption peak of the SiO_2 substrate. A comparison of the two spectra when normalized to 1 (Fig. S2 inset) shows that the resonance peaks of the measured BiMIM structure can be clearly resolved even in the raw untreated spectrum, showing the efficacy of the IR-SMS technique.
The polarized thermal emission spectra presented in Fig. 3(a) of the main text, were obtained by adding a BaF_2 wire grid polarizer– with maximum transmission in the measured spectral range– before the detector.

2. FDTD SIMULATIONS

The simulations presented in the main text where performed using FDTD calculations (Lumerical solutions). In order to simulate an isolated BiMIM structure perfectly matched layers (PMLs) were effected for all boundaries. Unpolarized, normally incident, broadband electromagnetic radiation in the 6-13 μm range was used as the source of excitation. The simulation span was made large enough so that the distance between the edges of the patch antennas of the BiMIM structure and the PMLs was at least $\lambda/4$ in all directions, where λ is the maximum wavelength in the considered spectral range. This was done to reduce reflections by the PML boundaries and to improve the convergence of the simulations. The simulation time was also set large enough to insure proper convergence of all simulations. The emission cross-section was obtained by calculating losses due to absorption from the MIM antennas.
Palik data [5] were used in the simulations for the dielectric function of the gold layers. On the other hand, dielectric data reported in Ref. [4] for SiO_2 thin films were used for the SiO_2 layer. In order to estimate the difference between the used dielectric data for SiO_2 and the real one, we measured the thermal emission from the substrate, by collecting thermal radiation from a part of the sample that does not include any gold patches, using a mechanical chopper. The measured thermal emission of the substrate can be compared to the absorption of the SiO_2 layer, represented by the imaginary part of its index of refraction. As shown in Fig.S3 (a) the peak of absorption of the imaginary part of the index of refraction agrees well with the peak of the measured thermal emission.

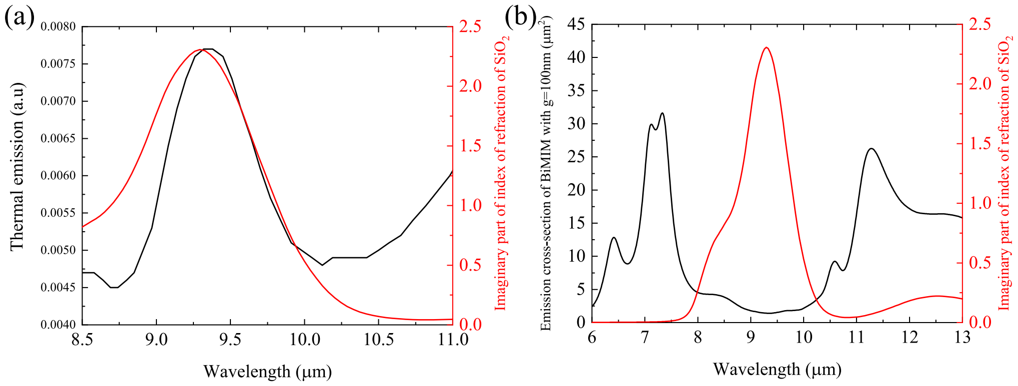

Fig. S3. (a) Measured thermal emission of the sample substrate, along with the imaginary part of the index of refraction of SiO_2 (taken from Ref. [4]) representing the absorption due to the substrate. (b) Simulated emission cross-section of a BiMIM structure for gap size $g = 100$ nm (black curve) presented in the main text (red curve in Fig. 2 (b) of the main text), along with the imaginary part of the SiO_2 index of refraction (red curve). The comparison of the two shows a high absorption due to SiO_2 in the spectral region between 8 and 13 μm, which prevents the formation of a splitting in the BiMIM emission spectrum in this range.

On examining the imaginary part of the index of refraction further, we find that due to the high absorption of SiO_2 in the spectral range between 8 and 13μm, a splitting due to the hybrid modes does not occur in this region. Indeed, as illustrated in Fig.S3 (b) the imaginary part of the index of refraction is zero in the spectral range where the splitting occurs (below $\sim$7.5 μm), while it is non-zero for higher wavelengths.

REFERENCES

1. C. Li, V. Krachmalnicoff, P. Bouchon, J. Jaeck, N. Bardou, R. Haidar, and Y. De Wilde, "Near-field and far-field thermal emission of an individual patch nanoantenna," Phys. Rev. Lett. **121**, 243901 (2018).
2. H. E. Revercomb, H. Buijs, H. B. Howell, D. D. LaPorte, W. L. Smith, and L. Sromovsky, "Radiometric calibration of ir fourier transform spectrometers: solution to a problem with the high-resolution interferometer sounder," Appl. Opt. **27**, 3210–3218 (1988).
3. H. Kallel, J. Doumouro, V. Krachmalnicoff, Y. De Wilde, and K. Joulain, "Thermal emission from a single glass fiber," J. Quant. Spectrosc. Radiat. Transf. **236**, 106598 (2019).
4. J. Kischkat, S. Peters, B. Gruska, M. Semtsiv, M. Chashnikova, M. Klinkmüller, O. Fedosenko, S. Machulik, A. Aleksandrova, G. Monastyrskyi *et al.*, "Mid-infrared optical properties of thin films of aluminum oxide, titanium dioxide, silicon dioxide, aluminum nitride, and silicon nitride," Appl. optics **51**, 6789–6798 (2012).
5. D. P. Edward and I. Palik, "Handbook of optical constants of solids," (1985).